Research Article | Vol. 24, No. 17 | 22 Aug 2016 | OPTICS EXPRESS 19366

Optics EXPRESS

Wavelength independent all-fiber angle-tunable polarization rotator based on geometric effects

ILKYU HAN* AND BYOUNG YOON KIM

Department of Physics, Korea Advanced Institute of Science and Technology, 291, Daehak-ro, Yuseong-gu, Daejeon, 34141, South Korea
**hanik@kaist.ac.kr*

Abstract: We propose and demonstrate a simple wavelength independent all-fiber polarization rotator based on purely geometric effects. The device rotates the orientation of an arbitrary input polarization state by arbitrary angle without changing other parameters of the polarization state. The device structure maintains inherent wavelength independence during the tuning process when a non-birefringent single-mode fiber is used.

OCIS codes: (060.2310) Fiber optics; (060.2340) Fiber optics component.

References and links

1. I. Han, J. Ko, and B. Y. Kim, "All-fiber variable polarization rotator based on geometric effects," in *2015 Conference on Lasers and Electro-Optics Pacific Rim,* (Optical Society of America, 2015) paper 28F2–4.
2. H. C. Lefevre, "Single-mode fibre fractional wave devices and polarization controllers," Electron. Lett. **16**(20), 778–780 (1980).
3. M. Johnson, "In-line fiber-optical polarization transformer," Appl. Opt. **18**(9), 1288–1289 (1979).
4. A. Starodoumov and P. Crittenden, "Double-pass fiber amplifier," United States patent 7440181 (Oct. 21, 2008).
5. F. J. Duarte, "Optical device for rotating the polarization of a light beam," United States patent 4822150 (Apr. 18, 1989).
6. K. Jain, "Polarization rotation method and apparatus," United States patent 4252410 (Feb. 24, 1981).
7. R. Ulrich, S. C. Rashleigh, and W. Eickhoff, "Bending-induced birefringence in single-mode fibers," Opt. Lett. **5**(6), 273–275 (1980).
8. E. Hecht, *Optics* (Addison Wesley, 2002).
9. M. V. Berry, "Quantal phase factors accompanying adiabatic changes," Proc. R. Soc. Lond. A Math. Phys. Sci. **392**(1802), 45–57 (1984).
10. J. H. Hannay, "Angle variable holonomy in adiabatic excursion of an integrable Hamiltonian," J. Phys. Math. Gen. **18**(2), 221–230 (1985).
11. A. Khein and D. F. Nelson, "Hannay angle study of the Foucault pendulum in action-angle variables," Am. J. Phys. **61**(2), 170–174 (1993).
12. J. N. Ross, "The rotation of the polarization in low birefringence monomode optical fibres due to geometric effects," Opt. Quantum Electron. **16**(5), 455–461 (1984).
13. A. Tomita and R. Y. Chiao, "Observation of Berry's topological phase by use of an optical fiber," Phys. Rev. Lett. **57**(8), 937–940 (1986).
14. F. Wassmann and A. Ankiewicz, "Berry's phase analysis of polarization rotation in helicoidal fibers," Appl. Opt. **37**(18), 3902–3911 (1998).
15. P. Senthilkumaran, B. Culshaw, and G. Thursby, "Fiber-optic Sagnac interferometer for the observation of Berry's topological phase," J. Opt. Soc. Am. B **17**(11), 1914–1919 (2000).
16. P. Senthilkumaran, "Berry's phase fiber loop mirror characteristics," J. Opt. Soc. Am. B **22**(2), 505–511 (2005).
17. R. Ulrich and A. Simon, "Polarization optics of twisted single-mode fibers," Appl. Opt. **18**(13), 2241–2251 (1979).

1. Introduction

We propose and demonstrate a novel variable polarization rotator based on purely geometric effect that maintains inherent wavelength independence during the tuning process. The work described in this paper solves a critical problem in the earlier report by the authors [1] by incorporating a mechanism that automatically compensates the birefringence induced by the tuning process. As a result, we could demonstrate much improved performance in terms of maintaining the linearity of the input linear polarization.

#269460 http://dx.doi.org/10.1364/OE.24.019366
Journal © 2016 Received 29 Jun 2016; revised 5 Aug 2016; accepted 8 Aug 2016; published 11 Aug 2016

Optics EXPRESS

Polarization control is critical in many optical systems especially in fiber optic circuits where random birefringence in a long fiber is inevitable due to external perturbations as well as intrinsic imperfections. For this reason, various forms of fiber optics polarization controllers are utilized in typical fiber systems to control polarization state of light at certain position in the fiber [2, 3]. While the polarization controllers are very convenient to use, most of them do not provide the information on the exact action of the device to the input polarization without analyzing the state of polarization at the output. For many optical systems such as double-pass amplifiers [4], a simple polarization rotator by 90 degrees without changing other polarization parameters is needed. For optical systems where simple rotation of polarization is required, half-wave plates, Faraday rotators, Fresnel rhombs, prisms and mirrors can be used [4–6]. The half-wave plates in both bulk optic and fiber optic form have wavelength dependence in addition to the reversal of sense of rotation for elliptical polarizations [7]. Faraday rotators also exhibit wavelength dependence [8]. Fresnel rhombs, prisms and mirrors do not have wavelength dependence but they do not provide simple means to tune the rotation angle and would not be convenient to use in fiber optic systems [5, 6].

In classical and quantum mechanics, when a system experiences cyclic adiabatic processes, it memorizes the path by phase difference which is called the geometric phase or Berry phase [9]. The Hannay angle of the Foucault pendulum is the most representative example [10, 11]. Polarization rotation in a single-mode optical fiber helically wound on a cylinder is also an example of the geometric phase. In this case, the orientation of the output polarization rotates in proportion to the pitch length and the total length of the helix, and inversely proportional to the square of the arc length of one helix turn [12–16]. This effect can be used for polarization rotation, but it still has wavelength dependence due to the bend-induced birefringence in the helically wound fiber. To eliminate the net bend-induced birefringence, we proposed and demonstrated a polarization rotator design with two discs [1]. However, the device could not be completely free from bend-induced birefringence when the rotation angle is tuned away from the optimal value. The device structure in this report solves the problem by adding a specially designed disc that allows the wavelength independent polarization rotation. The added disc rotates and slides to counteract the bent fiber length change induced when the polarization angle is rotated. As a result, the total bend-induced birefringence in the device is maintained at the initially designed zero value and therefore provides wavelength independent operation.

2. Fixed polarization rotator

2.1 Experimental setup

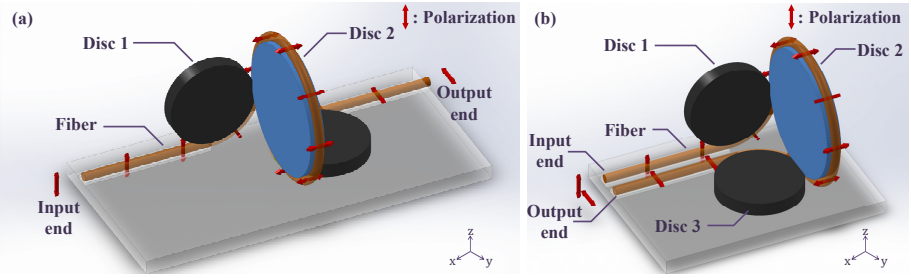

Fig. 1. Structure of the polarization rotator. (a) Collinear type, (b) Reflector type.

First, we describe two different forms of polarization rotator with fixed 90 degrees rotation angle as shown in Fig. 1. The polarization rotator consists of three discs. The discs 1 and 3 are attached to the left and the bottom edge of the disc 2, respectively. To rotate the orientation of polarization by 90 degrees, the angle between the two attaching points should be at right angle on the disc 2. A non-birefringent single-mode fiber is wound around the circumference of each disc as shown in Fig. 1. In order to avoid unwanted twist-induced birefringence, care

Optics EXPRESS

has to be taken so that the fiber does not experience torsional stress at any point in the fiber [17].

Note that the fiber is wound for the arc angles of 90 degrees for the discs 1 and 3 having the same diameter, and 270 degrees for the disc 2 in both the collinear and reflection type configurations. Also note that the input polarization aligned with the fast (slow) axis of the bend-induced birefringence in the disc 1 will be aligned with the fast (slow) axis in the disc 3, while it is aligned with the slow (fast) axis in the disc 2. This is illustrated as red arrows in the figure. It is well known that the bend-induced birefringence β_b is expressed as follows [7]:

$$\beta_b(R) = \frac{n^3}{4} k (p_{11} - p_{12})(1+\nu)\frac{r^2}{R^2}, \tag{1}$$

where n is refractive index of core, k is the propagation constant in the vacuum, p_{ij} denote the strain-optical coefficients, ν is the Poisson's ratio, r is the fiber radius, and R is the bend radius. If the radius of the discs 1 and 3 is R_1 and the radius of the disc 2 is R_2, then the net phase difference $\Delta\varphi$ between the two polarizations after propagating through the device is given by

$$\Delta\varphi = \frac{\pi n^3}{4} k (p_{11} - p_{12})(1+\nu) r^2 \left(\frac{1}{R_1} - \frac{3}{2}\frac{1}{R_2} \right). \tag{2}$$

We designed so that the net bend-induced birefringence in the device to be completely canceled by making the diameter of the disc 2 be 1.5 times that of the discs 1 and 3. In the experiment, the diameter of the discs 1 and 3 was 3 cm and that of the disc 2 was 4.5 cm.

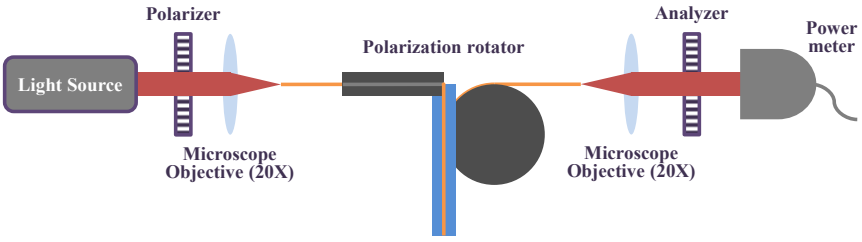

Fig. 2. Experimental setup.

The experimental setup to evaluate the performance of polarization rotation is shown in Fig. 2. We used three different light sources (a He-Ne laser at 633 nm, a laser diode at 977 nm, and a tunable laser at 1515–1595 nm) to measure the wavelength dependence of the polarization rotator. In order to launch linear polarization with different angles at the input, a glass polarizer was placed between the light source and the microscope objective. Three different low birefringence optical fibers that are single-moded at the three wavelengths are used for the test. The fiber length in the device was 35 cm except for the case of 977 nm wavelength. For the wavelength of 977 nm, an extra length of 50 cm at the end was required to completely eliminate the cladding mode. The output polarization was analyzed with an analyzer having a polarization extinction ratio of greater than 40 dB.

2.2 Experimental results

First, we measured the rotation angle of linear polarization for three different input polarization states (0, 90, and 135 degrees with respect to optical table) with a He-Ne laser. The experimental results are summarized in Table 1. The polarization extinction ratio (PER) is the ratio of the minimum intensity to the maximum intensity when the analyzer angle is rotated which indicates how well the linear polarization is maintained through the device.

Optics EXPRESS

It can be seen that the device provides good performance for both the rotation angle and the maintenance of linearity of the linear polarization. The measurement error for the polarization angle was ± 2 degrees in the experimental setup. For the vertical polarization (90°) input, the PER was larger than 38.7 dB that was limited by the sensitivity of the detector. The PER for the diagonal polarization angle was measured to be 25.2 dB. It is lower than other cases and we believe it is caused by small intrinsic birefringence in the fiber. We measured intrinsic linear birefringence before winding the fiber on the device. The value of intrinsic linear birefringence β is 1.03 rad/m. In the worst case this amount of birefringence in a 35 cm-long fiber can result in the PER of 14.8 dB when its two birefringence axes are excited equally.

Table 1. Performance of the polarization rotator at 633 nm wavelength.

Input polarization orientation (deg)	*0*	*90*	*135*
Rotated angle of polarization (deg)	90	88	88
Polarization extinction ratio (dB)	37.3	> 38.7	25.2

We carried out further experiments using light sources and fibers for different wavelengths in the setup in Fig. 2 to measure the wavelength dependence and Table 2 shows the experimental results. The input linear polarizations were vertically (90°) and diagonally (135°) oriented with respect to the optical table. The experimental results confirm wavelength independent operation over a very wide wavelength span that cannot be achieved with conventional devices having non-zero net birefringence. One thing to note is that the relatively low PER for the wavelength of 977 nm is believed to be due to the intrinsic birefringence of the fiber. The amount of intrinsic linear birefringence β was measured to be 0.648 rad/m that can produce the worst case PER of 11.0 dB for an 85 cm-long fiber

Table 2. Wavelength dependence of the polarization rotator.

Input polarization orientation (deg.)	*90*		*135*	
Wavelength (nm)	*Rotated angle of polarization (deg)*	*Polarization extinction ratio (dB)*	*Rotated angle of polarization (deg)*	*Polarization extinction ratio (dB)*
632.8	90	> 38.7	88	25.2
977.0	89	17.4	92	17.3
1535	90	25.1	91	> 32.9
1550	90	> 37.5	89	> 34.2
1565	91	25.9	88	> 32.5

3. Variable polarization rotator

3.1 Experimental setup

In our earlier report [1], the tuning of polarization rotation angle was achieved by rotating a disc to which a second disc is attached as shown in part of Fig. 3 (discs 2 and 3). However, as the disc 2 is rotated, the net bend-induced birefringence deviates from the originally designed zero value. The addition of the disc 1 having the same radius (R_1) as that of the disc 2 in Fig. 3 provides a novel solution to this problem by automatically compensating the added

Optics EXPRESS

birefringence due to the rotation of the disc 2. As shown in Fig. 3(a), the disc 1 can rotate on its axis that can linearly translate towards the disc 2. Detailed structure of the disc 1 with fiber arrangement is shown in Fig. 3(b).

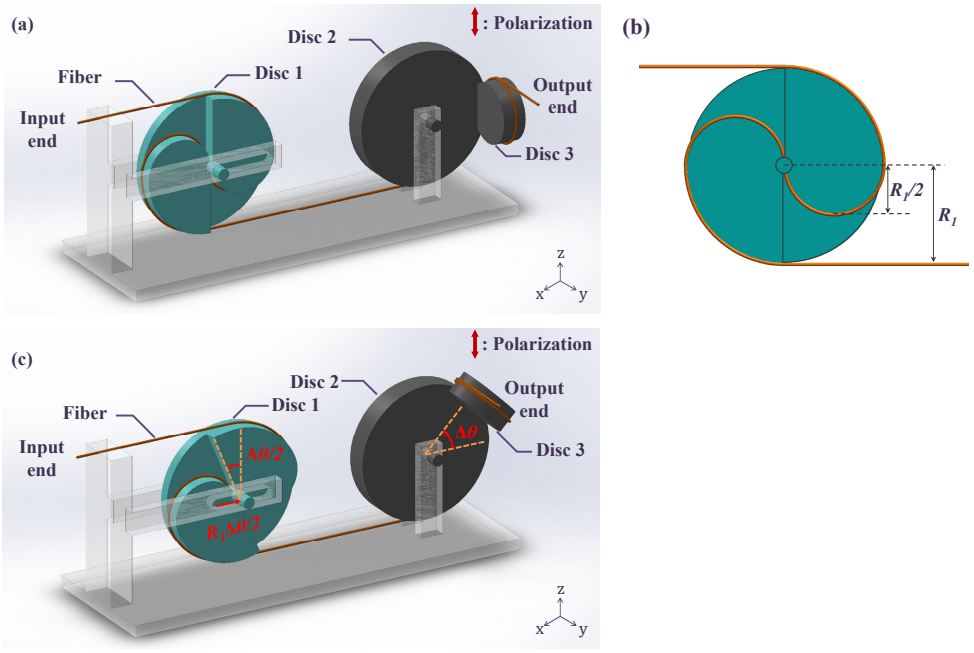

Fig. 3. Variable polarization rotator. (a) Arrangement for 90° rotation. (b) Side view of the disc 1 for 90° rotation. (c) Arrangement for $90^\circ + \Delta\theta$ rotation.

The discs 2 and 3 are attached at the edge with 90 degrees angle and the disc 2 is rotatable. The output polarization is rotated if the disc 2 is rotated as described in detail in [1], Han et al. At the same time the fiber length wound on the disc 2 changes resulting in the change of net bend-induced birefringence by the disc 2. As depicted in Fig. 3(c), when the disc 2 is rotated by $\Delta\theta$ counterclockwise to rotate the output polarization by the same angle, the same fiber length will be unwound from the disc 1 and the total change in net birefringence remains at zero value. In this operation, the disc 1 rotates counterclockwise by $\Delta\theta/2$ and translates toward the disc 2 by $R_1\Delta\theta/2$.

The bend-induced birefringence on the disc 3 has to be the same magnitude with opposite sign of the combined bend-induced birefringence from the discs 1 and 2. For this, the radius of the disc 3 is determined to be $(5/11)\cdot R_1$ with $5/4$ turns of fiber wound around the disc 3. The diameters of the discs used in the experiment were 6 cm for discs 1 and 2, and 2.73 cm for the disc 3.

Optics EXPRESS

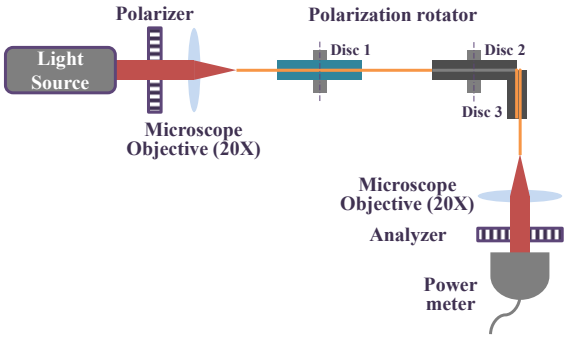

Fig. 4. Experimental setup.

Figure 4 shows the experimental setup to measure polarization rotation performance. We used a distributed feedback laser diode as a light source at 1550 nm. The glass polarizer after the light source ensures that the incident beam is linearly polarized. The linearly polarized beam was launched into the single-mode fiber using a microscope objective. The length of the fiber in the device was 46 cm. The state of polarization of output beam was analyzed with an analyzer and a power meter. The PER of the polarizers was better than 40 dB at 1550 nm wavelength.

3.2 Experimental results

We observed the output polarization for two different input polarizations and two rotation angles. The input beams were linearly polarized. One was vertical (90°) and the other was diagonal (135°) to optical table. Rotation angles of the variable polarization rotator were 90 and 135 degrees. The experimental results are summarized in Table 3.

Table 3. Performance of the Variable Polarization Rotator.

Input polarization orientation (deg.)	*90*		*135*	
Rotation angle of polarization rotator (deg.)	*90*	*135*	*90*	*135*
Rotated angle of polarization (deg.)	89	135	89	134
Polarization extinction ratio (dB)	> 30.1	> 29.1	> 30.3	> 29.2

From the experimental results, we can confirm that the variable polarization rotator provides high performance independent of rotation angle and wavelength as we predicted. The PER value in Table 3 was limited by the sensitivity of the detector used

4. Conclusion

We proposed and demonstrated a novel wavelength independent all-fiber polarization rotator based on geometric effect for fixed and tunable rotation angles. The experimental results with different input polarization angles, polarization rotation angles, and operating wavelengths showed high performance in terms of angle accuracy, PER, and wavelengths independence. The demonstrated device has a simple structure and may be useful for various fiber optic systems

Funding

National Research Foundation of Korea (NRF) (2013R1A1A2064061).